# Push-Pull and Conventional Nitriles as Halogen Bond Acceptors in their Cocrystals with Iodo-substituted Perfluorobenzenes

Yulia N. Toikka,[1] Rosa M. Gomila,[2] Antonio Frontera,[2] Yulia A. Izotova,[1]

Vadim Yu. Kukushkin,*[1,3] Nadezhda A. Bokach*[1]

[1] *Institute of Chemistry, Saint Petersburg State University, 7/9 Universitetskaya Nab., Saint Petersburg 199034, Russian Federation*

[2] *Department of Chemistry, Universitat de les Illes Balears, Crta de Valldemossa km 7.5, 07122 Palma de Mallorca (Baleares), Spain*

[3] *Laboratory of Crystal Engineering of Functional Materials, South Ural State University, 76 Lenin Av., Chelyabinsk 454080, Russian Federation*

*Corresponding authors

**Abstract**. Co-crystallization of the push-pull nitriles $NCNR_2$ ($R_2$ = $Me_2$ **1**, $C_4H_8$ **2**, $C_5H_{10}$ **3**, $C_4H_8O$ **4**) with iodo-substituted perfluorobenzenes (1,4-diiodotetrafluorobenzene – 1,4-FIB and 1,3,5-triiodotrifluorobenzene – 1,3,5-FIB), gave cocrystals **1**·1,3,5-FIB, **2**·1,3,5-FIB, **3**·½(1,4-FIB), **4**·½(1,4-FIB), and **4**·2(1,3,5-FIB), which were studied by single-crystal X-ray diffractometry (XRD). The structure-directing I···*sp*-$N_{nitrile}$ halogen bond (HaB) in all cocrystals was identified based on the consideration of the XRD geometrical (bond length and angles) parameters and also by Hirshfeld surface analysis, whereupon the observed HaBs were analyzed theoretically. The HaB accepting role of the push-pulling dialkylcyanamides $NCNR_2$ and conventional nitriles NCR (R = Alk) was examined and compared in details using, as model examples, the structures of cocrystals **3**·½(1,4-FIB) (this work) and AdCN·½(1,4-FIB) (CSD refcode: KIHROL). These two cocrystals, which display similar supramolecular organization, were studied by several quantum chemistry methods including molecular electrostatic potential (MEP) surface analysis, the natural bond orbital (NBO) analysis, the quantum theory of atoms in molecules (QTAIM) combined with and NCIPlot approach, and also by the Kitaura–Morokuma energy decomposition approach. While AdCN is slightly poorer *sp*-N electron donor than the push-pull nitrile **3**, HaBs in the cocrystals exhibit similar interaction energies. Although in the covalent chemistry, the two types of nitriles often exhibit strikingly different reactivity patterns, the σ-hole based I···*sp*-$N_{nitrile}$ noncovalent interaction provided the leveling effect resulting in significant similarities between the HaB situations for both nitrile species.

## 1. Introduction

Although halogen bonding (abbreviated as HaB) is a recognized phenomenon since Hassel Nobel lecture (1970),[1] it was defined by IUPAC only in 2013.[2-3] Several highly cited reviews, that appeared in the past decade, summarized the theoretical and experimental approaches allowing for HaB identification and also highlighting various areas of its application.[4-14] Recent surveys focused on HaB demonstrate its use in organocatalysis,[15-16] crystal engineering,[17-19] fabrication of functional materials,[20-25] sensing,[18, 26-27] and drug design.[28]

According to the IUPAC definition,[2] in a HaB the electrophilic region of a halogen atom (σ-hole; for reviews on σ-hole interactions see refs.[29-32]) attractively interacts with any nucleophilic region; the electrophilic region is not necessarily electropositive, but it should be less electronegative than the partner. These HaB *donors* commonly include nonmetal atoms bearing lone pairs, (e.g., O, N, halogen etc.[8]), π-bond(s)[8] systems (e.g., aromatic rings), and nucleophilic metal sites (e.g., a $d_z^2$-nucleophilic $Pt^{II}$ site).[33] The most common group of HaB *acceptors* is represented by nitrogen-based nucleophiles[34] featuring $sp^3$-N (amines), $sp^2$-N (nitrogen heterocycles and imines), and *sp*-N sites. The former two groups exhibit a pronounced nucleophilicity and it is not unusual that they are often employed as acceptor components in HaB-involving crystal engineering. In particular, $sp^3$-amines (e.g., DABCO[35-36]) have been applied to verify main HaB patterns and the nature of these noncovalent forces.

The *sp*-N atom of various cyano groups (for example, RCN, $CN^-$ or $SCN^-$) can also serve as a HaB acceptor. However, its nucleophilicity and, consequently, HaB acceptor properties are significantly weaker than those for $sp^3$- and $sp^2$-N sites. Expectably, a number of studies—focused on HaB and including *sp*-N atoms as nucleophilic components—is rather small. In this context, one should mention cocrystals of 1,4-dicyanobutane and 1,6-dicyanohexane with diiodoperfluoroalkanes,[37] cocrystals formed between 1,4-bis-(*p*-cyanostryl)benzene and 1,4-disubstituted iodobenzenes,[38] differently iodo-substituted phthalonitriles and benzonitriles,[39-40]

featuring I···*sp*-N≡C HaBs in their crystal structures. A similar I···*sp*-N≡C HaB motif was also observed in the crystal structures of the copper(II) [Cu{$(OC)_2CC_6H_4C{\equiv}CI$-4}$_2$]·MeCN solvate[41] and the gold(I) isocyanide complex [Au($C_6H_4C{\equiv}N$-4)($C{\equiv}NC_6H_4I$-4)]. In the latter structure, two remote sites (the I-atom and nitrile group in the 4$^{th}$ position) are halogen-bonded.[42]

The nature of the I···*sp*-N≡C contact was earlier studied by theoretical methods in comparison with other types of HaB. Scheiner[43] compared HaB involving *N*-bases of various *N*-hybridization and diverse C–X HaB donors (X = Cl, Br, I). The energetics of these systems is not much sensitive to the hybridization of the N atom but—according to the obtained binding energies—interactions are weakened in the order $sp^3 > sp^2 > sp$. Analysis of the wave functions within the atom-in-molecules (AIM) formalism demonstrated that the highest bond critical point (BCP) densities occur for adducts with the $NMe_3$ donor and they are weakest for the nitrile NCMe; the latter trend reflects weakening of appropriate HaBs ongoing from $sp^3$- to *sp*-N sites.

In this study, we compared *push-pulling* dialkylcyanamides $NCNAlk_2$ and *conventional* nitriles NCR (having Alk or Ar as R group) in their ability to function as HaB acceptors. Dialkylcyanamides belong to the category of push-pull nitriles, namely to highly polarized systems with the electronegative N atom on one side of the C≡N bond and an electron-donating $NR_2$ group (exhibiting an expressed +*M* effect) on the other side.[44] The n-π conjugation between the two ends of such systems lowers the basicity of the pushing amide-group(s) and increases the basicity of the pulling cyano group.[44] Dialkylcyanamides also exhibit a reactivity that differs from that observed for conventional nitriles at the quantitative and qualitative levels—as stated in experimental reports[45-47] and in a review by two of us.[48] A comparison of the push-pulling dialkylcyanamides and the conventional nitriles in their role of *sp*-N HaB acceptors has never been performed in the past and it comprises the goal of this study.

## 2. Results and Discussion

**2.1. The CSD search for $R_2NCN{\cdot}I{-}R$ adducts**. To obtain more data on the ability of the dialkylcyanamide cyano group to function as a HaB acceptor toward I- or Br-substituted organic species, we performed a Cambridge Structural Database (CSD) search for short C–Q···N≡CR separations (R = Alk, Ar, or NR'$_2$; Q is Br or I; Q–N distance is smaller than the corresponding Bondi $\Sigma_{wdW}$(Q + N); ∠C–Q–N is in the range 135–180°). Using these criteria, we retrieved 500+ structures and it is clear that it is difficult to analyze this large massive of structural data. Therefore, the search was restricted to only iodo- and bromo-fluoro(hetero)arenes including functionalized species. With these criteria 32 structures featuring $C_{ArF}$–Q···N≡C–R contacts were retrieved (R = Alk, Ar; no structures with R = $NR_2$ were found; **Table S1**).

Inspection of the data gathered in **Table S1** verified three structures, which are similar to dialkylcyanamide·FIB adducts (**section 2.2**), namely cocrystals MeCN·1,4-FIB·18-crown-6 (DUKREJ[49]), MesCN·$IC_6F_5$ (EBIHEF[50]), and 2AdCN·1,4-FIB (KIHROL[51]). All these structures demonstrate relatively short and rather directional I···N contacts (I···N distance 3.05–3.18 Å; ∠C–I···N 174–178°).

Next, another CSD search was conducted exclusively for cyanamides and related species exhibiting C–Q···N≡C–N contacts; seven structures with $R_w \leq 10\%$ were found (**Table S2**). Within the latter group, five structures are represented by cyanoimines, N≡CN=CRR', and one example is diazocyanide, N≡CN=NR. The only one structure featuring Br···N short contact relates to dialkylcyanamide (MEKWIL[52]). All these results indicate that HaB involving dialkylcyanamides as HaB acceptors is almost unexplored; we did not find even a single example of HaB with iodo- (or bromo) perfluoroarenes.

**2.2. Halogen-bonded cocrystals of dialkylcyanamides.** The push-pull nitriles $NCNR_2$ ($R_2$ = $Me_2$ **1**, $C_4H_8$ **2**, $C_5H_{10}$ **3**, $C_4H_8O$ **4**) and such iodo-substituted perfluorobenzenes as 1,4-

diiodotetrafluorobenzene (1,4-FIB) and 1,3,5-triiodotrifluorobenzene (1,3,5-FIB), were co-crystallized in a 3:1 molar ratio in acetonitrile solutions at 20–25 °C. In five cases, we isolated cocrystals suitable for X-ray diffraction (XRD), namely **1**·1,3,5-FIB, **2**·1,3,5-FIB, **3**·½(1,4-FIB), **4**·½(1,4-FIB), and **4**·2(1,3,5-FIB). Four obtained XRD structures were of rather good quality ($R_w$<5%) and the structure of **1**·1,3,5-FIB ($R_w$>5%) is not suitable for the accurate discussion of noncovalent interactions. However, the composition of the latter cocrystal was clearly established (**Figure S1**). Cocrystals **2**·1,3,5-FIB, **3**·½(1,4-FIB), **4**·½(1,4-FIB), and **4**·2(1,3,5-FIB) exhibit different cyanamide:FIB molar ratios and they demonstrate different supramolecular patterns. Examination of the ATR-IR spectra of all cocrystals revealed insignificant lower- or higher frequency shifts of ν(C≡N) as compared to the ν(C≡N) stretches of the parent complexes (**section S3**).

To identify noncovalent forces which provide a significant contribution to the crystal packing, we performed the Hirshfeld surface analysis. For visualization, we used a mapping of the normalized contact distance ($d_{norm}$) (**Figures 1** and **S13–S15**). The I···N contacts (in **3**·½(1,4-FIB), **2**·1,3,5-FIB, and **4**·2(1,3,5-FIB)) and the I···O contacts (in **4**·2(1,3,5-FIB) and **4**·½(1,4-FIB)) are clearly seen on the Hirshfeld surface of the dialkylcyanamides as red dots corresponding to short interatomic contacts (**Figure 1**).

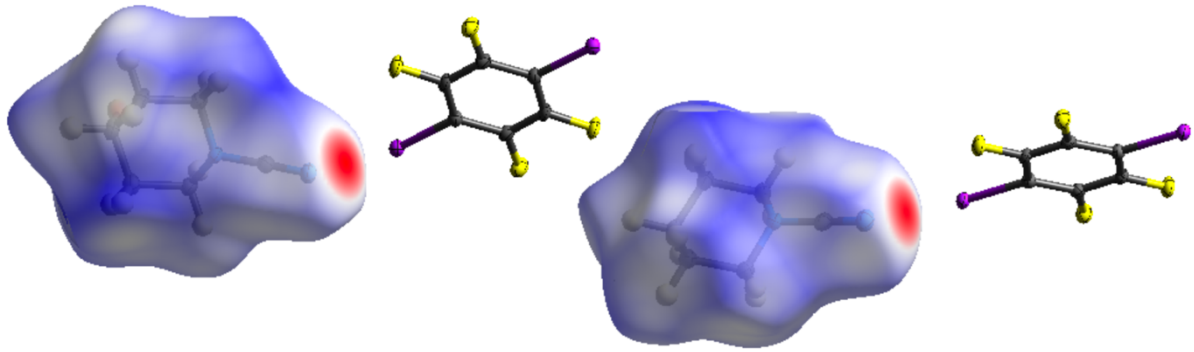

**Figure 1**. Hirshfeld surface of two crystallographically independent molecules **3** in the structure of **3**·½(1,4-FIB) mapped with $d_{norm}$ showing the I···N short contact.

In the structures of the cocrystals, we identified the following structure-directing interactions: I···N HaB occurred between a FIB iodine and the nitrile *sp*-N atom (**2**·1,3,5-FIB, **3**·½(1,4-FIB), and **4**·2(1,3,5-FIB)); I···O HaB between a FIB iodine atom and the morpholine entity (**4**·½(1,4-FIB), **4**·2(1,3,5-FIB)); I···I HaB between an iodine atom of 1,3,5-FIB (**4**·2(1,3,5-FIB) and **2**·1,3,5-FIB); LP(I)-π (LP is a lone pair) and/or parallel displaced π-π-stacking between the neighboring perfluoroarenes in all cocrystals, interactions between two nitrile groups of $NCNR_2$ (**3**·½(1,4-FIB) and **4**·½(1,4-FIB), and various types of weak hydrogen bonds such as C–H···F, C–H···N, C–H···O, and C–H···I (for comparison of HaB and hydrogen bonding see ref.[53] and references therein). The geometric parameters of these contacts are listed in **Tables 1** and **2**.

**Table 1**. Geometric parameters of the C–I···N, C–I···O, and C–I···I HaBs.

| Co-crystal | C–I···X | *d*(I···X), Å (Nc) | ∠(C–I···X),° | ∠(I···X–C),° |
|---|---|---|---|---|
| **2**·1,3,5-FIB | C1S–I1S···N1–C1 | 2.944(5) (0.83) | 171.56(19) | 128.8(4) |
| | C5S–I3S···N1–C1 | 3.148(4) (0.89) | 174.8(2) | 95.2(4) |
| | C3S–I2S···I1S–C1S | 3.9119(5) (0.99) | 176.10(17) | 116.45(13) |
| **3**·½ (1,4-FIB) | C1S–I1S···N1–C1 | 2.8990(19) (0.82) | 170.93(9) | 144.7(2) |
| | C4S–I2S···N3–C7 | 2.9402(18) (0.83) | 174.18(10) | 167.9(3) |
| **4**·½(1,4-FIB) | C1S–I1S···O1–C3/C4 | 2.9141(18) (0.83) | 171.33(10) | 104.78(13) |
| | | | | 124.17(14) |
| | C4S–I2S···O2–C8/C9 | 2.9144(18) (0.83) | 175.42(8) | 125.18(16) |
| | | | | 103.36(14) |
| **4**·2(1,3,5-FIB) | C6S–I3S···N1–C1 | 2.966(6) (0.84) | 173.78(15) | 158.5(4) |
| | C7S–I4S···N1–C1 | 3.140(5) (0.89) | 167.77(19) | 97.7(4) |

| | | | |
|---|---|---|---|
| C9S–I5S···O1–C3/4 | 2.826(4) (0.81) | 173.40(14) | 135.5(3) |
| | | | 113.5(3) |
| C4S–I2S···I5S–C9S | 3.8559(5) (0.97) | 170.02(16) | 109.62(14) |
| C2S–I1S···I3S–C6S | 3.7678(5) (0.95) | 168.08(13) | 110.97(15) |
| C11S–I6S···I5S–C9S | 3.8569(5) (0.97) | 160.77(13) | 109.27(15) |

Nc is normalized contact distance, Nc = d/$\sum_{vdW}$, where $\sum_{vdW}$ is Bondi[54] van der Waals radii sum for interacting atoms: $\sum_{vdW}$(I + O) = 3.50; $\sum_{vdW}$(I + N) = 3.53 Å; $\sum_{vdW}$(I + I) = 3.96 Å.

**Table 2**. Geometric parameters of stacking interactions.

| Cocrystal | Stacked moieties | Shortest *d*(X···Y), Å | Inter centroid *d*(Cg···Cg), Å |
|---|---|---|---|
| **2**·1,3,5-FIB | 1,3,5-FIB···1,3,5-FIB | C5S–I1S 3.773(5) | 4.584(5) |
| | LP(I)-π/π-π | C6S–C1S 3.799(8) | |
| **3**·½(1,4-FIB) | 1,4-FIB···1,4-FIB | C6S–I1S 3.608(3) | 4.327(2) |
| | LP(I)-π/π-π | C2S–C2S 3.775(4) | |
| | CN···CN | C7–N1 3.424(4) | |
| | | C1–N3 3.741(4) | |
| **4**·½(1,4-FIB) | 1,4-FIB···1,4-FIB | C5S–I1S 3.850(3) | 4.327(2) |
| | LP(I)-π/π-π | C6S–C1S 3.707(4) | |
| | CN···CN | C6–N1 3.201(4) | |
| | | C1–N4 3.336(4) | |
| **4**·2(1,3,5-FIB) | 1,3,5-FIB···1,3,5-FIB | C4S–I3S 3.791(4) | |
| | LP(I)-π | | |
| | 1,3,5-FIB···1,3,5-FIB | C12S–I5S 3.640(5) | 3.898(4) |

| | | |
|---|---|---|
| LP(I)-π/π-π | C10S–C8S 3.579(7) | |

Topicity of the FIBs and the directionality of donor/acceptor interactions as well as the nature of donor centers primarily determine the supramolecular architectures of the cocrystals. The cocrystals, which include the ditopic 180°-orienting 1,4-FIB (**3**·½(1,4-FIB) and **4**·½(1,4-FIB)), exhibit similar structural motifs consisting of HaB-based triads {**3**·1,4-FIB·**3**} and {**4**·1,4-FIB·**4**} – both linked by rather short HaBs (**Figure 2**).

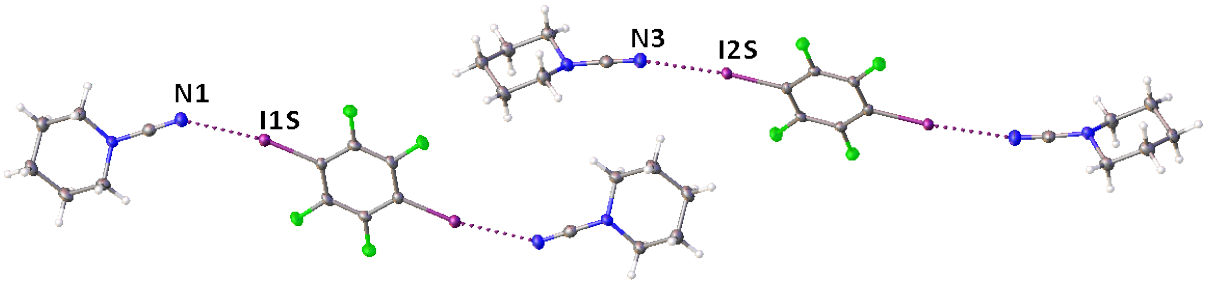


**Figure 2**. Two crystallographically independent HaB-based triads {**3**·1,4-FIB·**3**} in the structure of **3**·½(1,4-FIB). HaBs are shown by dotted lines.

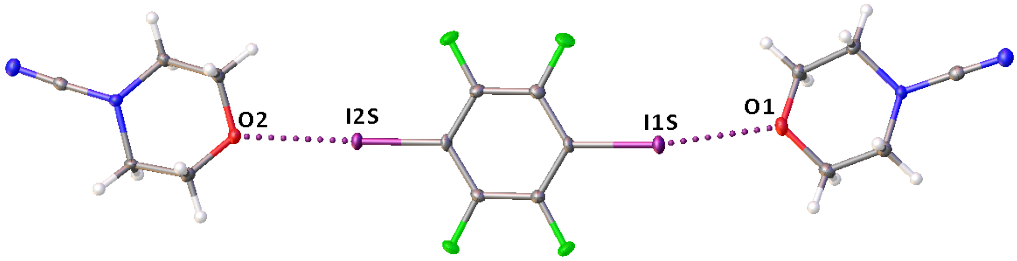


**Figure 3**. HaB-based triad {**4**·1,4-FIB·**4**} in the structure of **4**·½(1,4-FIB).

In **3**·½(1,4-FIB), the accepting center is the nitrile *sp*-N-atom, while in **4**·½(1,4-FIB) it is the O-atom of the morpholine entity. In the structure of **3**·½(1,4-FIB), triads {**3**·1,4-FIB·**3**} form the parallel displaced stacks between neighboring 1,4-FIBs. In turn, the stacks are linked to each other via the system of weak H-bonds and weak contacts between nitrile functionalities. Triads {**4**·1,4-FIB·**4**} (**Figure 3**) bearing the cyano groups, which are not halogen-bonded and form C–

H···$N_{nitrile}$ H-bonds and nitrile-nitrile contacts (**Figure 4**). Association of the neighboring 1,4-FIBs leads to the occurrence of π-π stacked dimers (for π-donor ability of 1,4-FIB see ref.[55]).

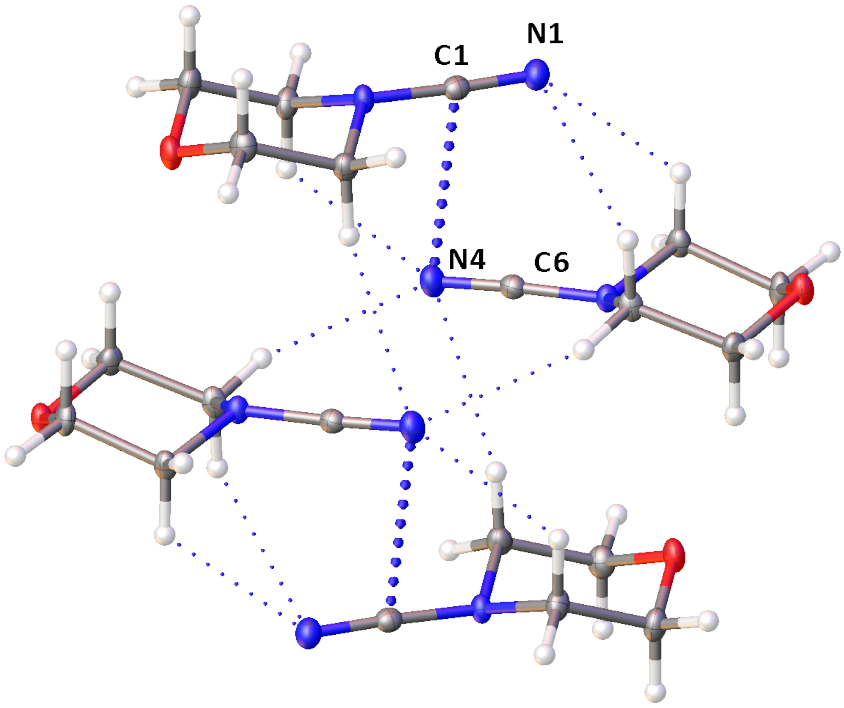


**Figure 4**. A fragment of the molecular structure of **4**·½(1,4-FIB) showing C–H···$N_{nitrile}$ HBs and nitrile-nitrile contacts; the shortest C···N separation is given by dotted lines.

The other two structures, **2**·1,3,5-FIB and **4**·2(1,3,5-FIB), include the tritopic planar 120°-orienting 1,3,5-FIB. Halogen-bonded pseudo-layers are formed via the combination of relatively strong I···N and I···O HaBs (only for **4**·2(1,3,5-FIB)) with weaker I···I (namely, σ-(I)-hole···iodine electron belt; for excellent review focused on halogen-halogen interactions see ref.[56]) HaBs (**Figures 5** and **6**).

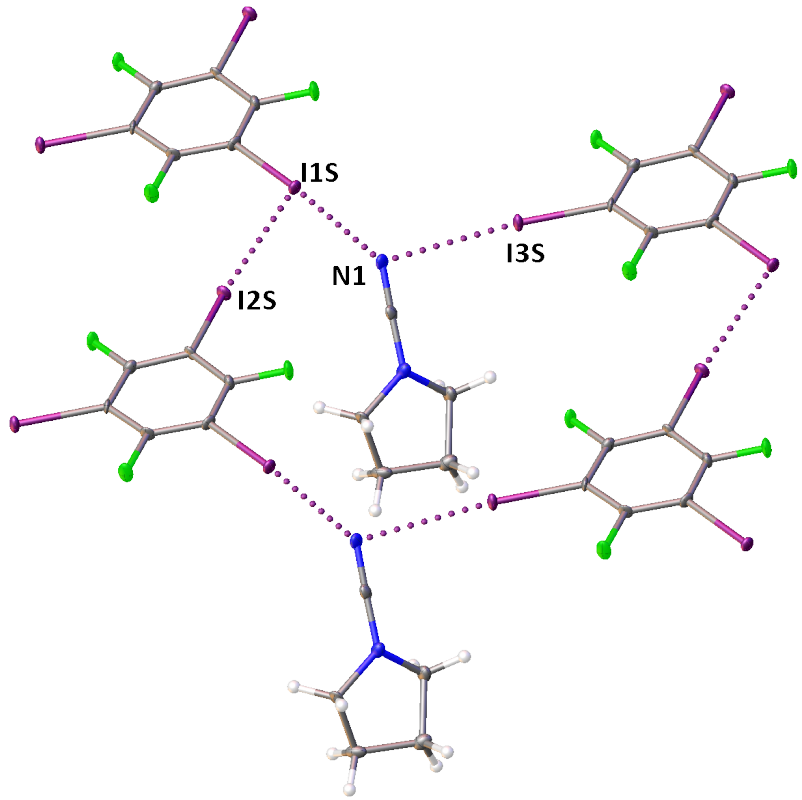


**Figure 5**. A fragment of the crystal structure of **2**·1,3,5-FIB showing I···N and I···I (dotted lines) HaBs.

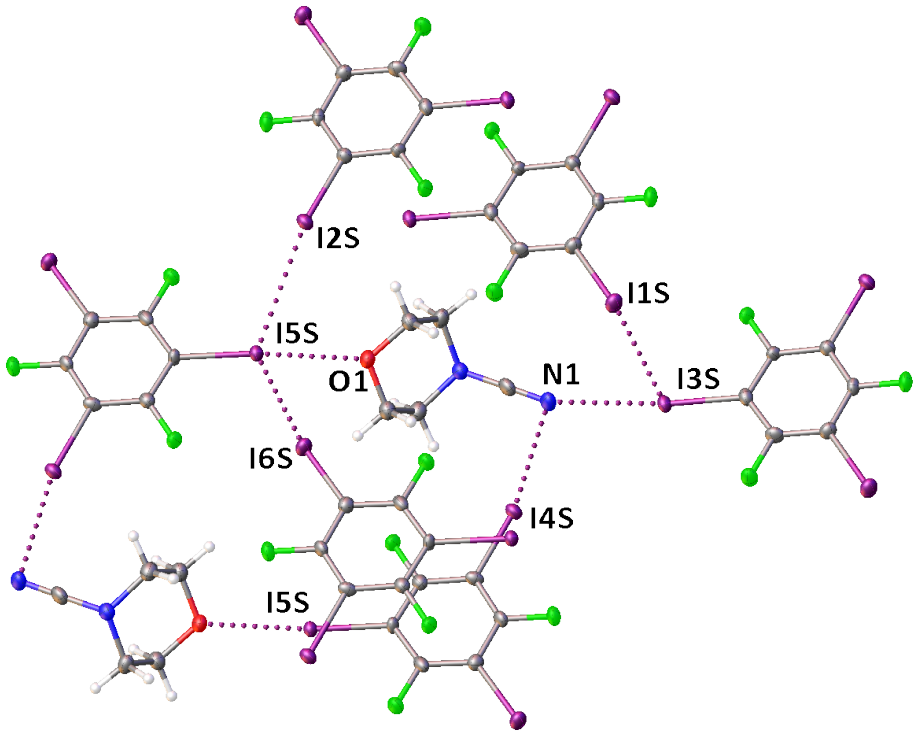


**Figure 6**. A fragment of the crystal structure of **4**·2(1,3,5-FIB) showing I···N, I···O, and I···I (dotted lines) HaBs.

These pseudo-layers are arranged in 3D-network via π-π stacking occurred between 1,3,5-FIB and a system of H-bonds.

**2.3. Comparison of I···N HaB in cocrystals including dialkylcyanamides and alkylnitriles.** To compare push-pulling dialkylcyanamides and alkylnitriles in their HaB accepting role, we choose the structures of **3**·½(1,4-FIB) (this work) and AdCN·½(1,4-FIB) (CSD refcode: KIHROL[51]). These structures exhibit a similar composition – both are bicomponent systems and contain the same ditopic HaB donor (1,4-FIB); they feature the same HaB donating:accepting coformers in a 1:2 ratio; and demonstrate similar supramolecular organization, namely the HaB-based triads {**3**·1,4-FIB·**3**} and {AdCN·1,4-FIB·AdCN} (**Figure 7**). The structure of **3**·½(1,4-FIB) contains two crystallographically independent triads {**3**·1,4-FIB·**3**}, which differ by their HaB parameters and $plane_{piperidine}$ to $plane_{1,4\text{-FIB}}$ angles (plane-to-plane twist angles are 158.94(15) and 79.29(12)°, plane-to-plane fold angles are 77.0(6) and 23.54(15)°, correspondingly; **Figure 7**).

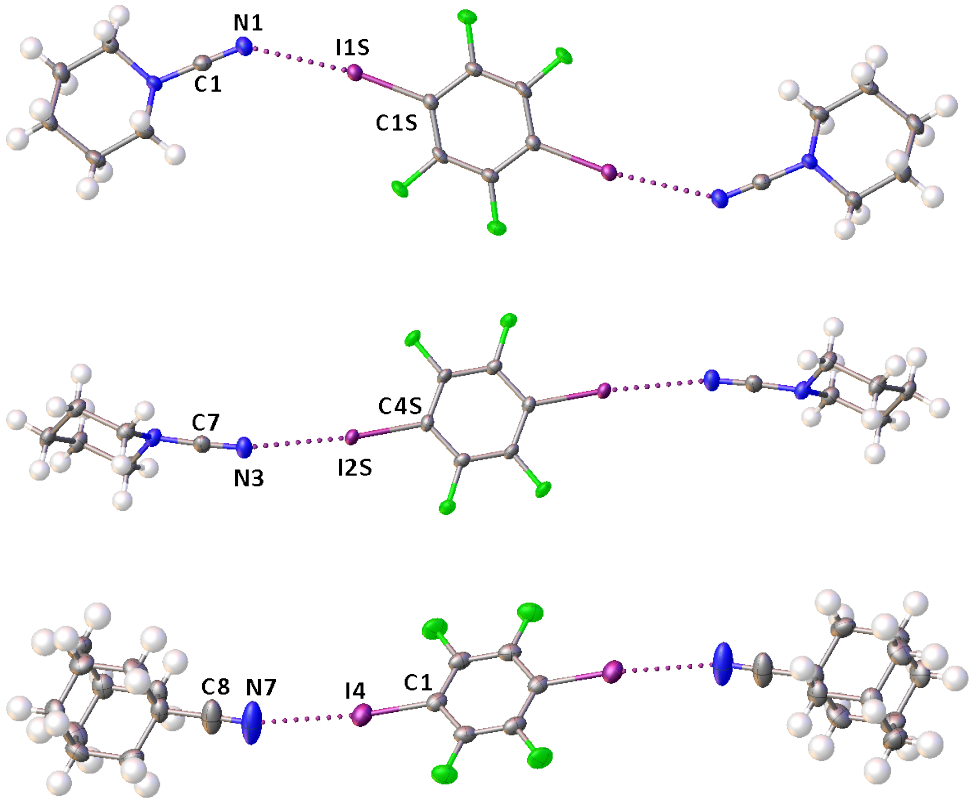


**Figure 7**. View of the HaB-based triads in the structures of **3**·½(1,4-FIB) (type A; top panel), **3**·½(1,4-FIB) (type B; middle panel), and AdCN·½(1,4-FIB) (bottom panel).

**Table 3**. Geometric parameters of C–I···N HaB in the studied cocrystals.

| Co-crystal | C–I···N | *d*(I···N), Å (Nc) | ∠(C–I···N),° | ∠(I···N–C),° |
|---|---|---|---|---|
| **3**·½ (1,4-FIB) | C1S–I1S···N1–C1 | 2.8990(19) (0.82) | 170.93(9) | 144.7(2) |
| | C4S–I2S···N3–C7 | 2.9402(18) (0.83) | 174.18(10) | 167.9(3) |
| AdCN·½ (1,4-FIB) | C1–I1···N1–C4 | 3.050(5) (0.86) | 173.88(10) | 167.43(10) |

**2.4. Theoretical study.** As indicated in **section 2.3**, the **3**·½(1,4-FIB) and AdCN·½(1,4-FIB) cocrystals exhibit similar supramolecular organization in the solid state (**Figure 7**). This result of the noncovalent pairing is somewhat unexpected considering that the reactivity of cyanamides and nitriles is in many instances strikingly different.[48] This theoretical study is focused on the comparative analysis of the HaB assemblies in **3**·½(1,4-FIB) and AdCN·½(1,4-FIB) cocrystals.

First, we computed the MEP surfaces of **3** and AdCN to compare the relative basicity of both compounds (**Figure 8**). The MEP minimum is indeed located at the *sp*-hybridized N-atom in both compounds (–46.4 and –42.7 kcal/mol in **3** and AdCN, respectively). The difference is small, thus suggesting that the electron donor ability of both molecules is similar but expectedly slightly larger for the cyanamide derivative. The MEP at the endocyclic N-atom in **3** is significantly less negative (–11.3 kcal/mol) due to the conjugation of LP with the cyano group. In both nitriles, the MEP maximum is located at the aliphatic H-atoms (+18.8 and +14.2 kcal/mol in **3** and AdCN, respectively).

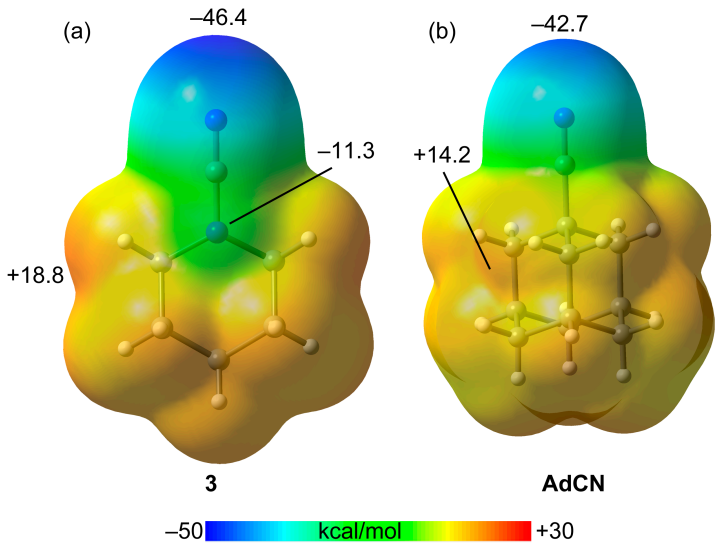


**Figure 8**. MEP surfaces of compounds **3** and AdCN at the PBE0-D4/def2-TZVP level of theory. Isodensity 0.001 a.u.

The unexpected small difference in the MEP minimum values of **3** and AdCN is likely due to the electron donation capability of the adamantyl group to the CN group by hyperconjugation of the three CC bonds in α-position similar to the donation of the endocyclic N-atom in **3** to the cyano group. This was corroborated using the natural bond orbital (NBO) analysis (**Figure S16**), where the conjugation of the endocyclic N-atom in **3** was compared to the hyperconjugation in AdCN. The conjugation in **3** is revealed by the NBO as a LP(N)→π*(C≡N) charge transfer with a concomitant second order stabilization energy of $E^{(2)}$ = 34.5 kcal/mol (**Figure S16b**). Obviously, the effect of the conjugation in **3** is larger than the sum of the three σ(C–C)→π*(C≡N) contributions (only one is represented in **Figure S16a**), that is 24.2 kcal/mol. However, the latter is surprisingly large and useful to justify the large and negative MEP value at the N-atom of AdCN.

To rationalize the formation of equivalent assemblies in **3**·½(1,4-FIB) and AdCN·½(1,4-FIB) cocrystals, we studied the trimers, shown in **Figure 7**, energetically and analyzed them by using the quantum theory of atoms in molecules (QTAIM) and NCIPlot methods based on the topology of the electron density. The results are gathered in **Figure 9** showing that all three assemblies exhibit similar interaction energies ranging from –9.4 to –10.4 kcal/mol. In the cases

of type A and B assemblies, they are basically isoenergetic thus suggesting that the HaB interaction energy is not sensitive to moderate changes in the I···N≡C angle. The trimeric assembly in the structure of AdCN·½(1,4-FIB) is slightly less energetically favorable (–9.4 kcal/mol), in line with the MEP surface analysis and also the occurrence of the trimers in the solid state.

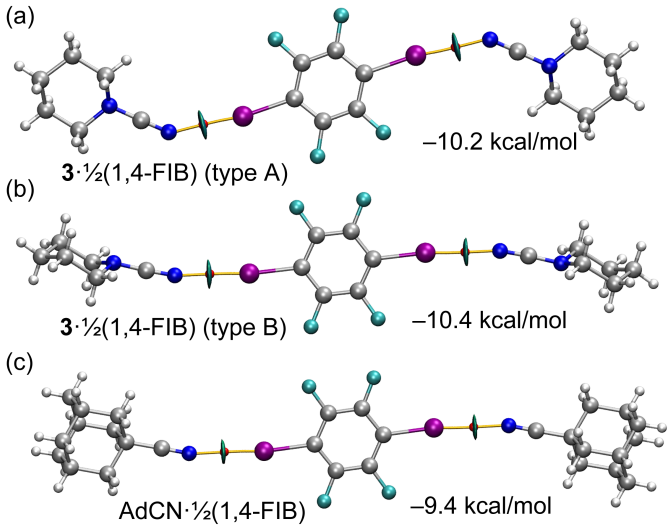


**Figure 9**. QTAIM (bond CPs in red and bond paths as solid lines) and NCIplot (see theoretical methods for settings) of **3**·½(1,4-FIB) type A (a), **3**·½(1,4-FIB) type B (b), and AdCN·½(1,4-FIB) (c) cocrystals. Only intermolecular contacts are shown. The interaction energies are also indicated.

Each HaB is characterized by a bond CP and bond path connecting the N-atom to the I-atom of the FIB molecule. Moreover, a bluish disk shaped RDG (reduced density gradient) isosurface also characterizes the HaB interaction. **Table 4** summarizes the QTAIM parameters at the bond CPs, showing the values, which are typical for noncovalent interactions: small charge density values ($\rho < 0.02$ a.u.), positive Laplacian ($\nabla^2\rho > 0$), and positive total energy density values ($Gr > |Vr|$). The energy associated to each HaB was also estimated using the Vr energy predictor and the equation $E = 0.68 \cdot Vr$, proposed in the literature.[57] The energies are in quite good agreement with half the binding energies provided in **Figure 9** for **3**·½(1,4-FIB) and AdCN·½ (1,4-FIB) trimers.

**Table 4**. QTAIM parameters at the bond CPs that characterize the C–I···N HaB in **3**·½(1,4-FIB) type A, **3**·½(1,4-FIB) type B, and AdCN·½(1,4-FIB) cocrystals. The interaction energies using the Vr energy predictor are indicated. In parenthesis half the energies computed for the trimers using the supramolecular approach are indicated)

| Co-crystal | ρ | G(r) | V(r) | H(r) | $\nabla^2\rho$ | $E_{int}$ |
|---|---|---|---|---|---|---|
| **3**·½(1,4-FIB) | | | | | | |
| **type A** | 0.0198 | 0.0147 | –0.0134 | 0.0013 | 0.0638 | –5.7 (–5.1) |
| **type B** | 0.0184 | 0.0138 | –0.0123 | 0.0015 | 0.0610 | –5.2 (–5.2) |
| AdCN·½(1,4-FIB) | 0.0148 | 0.0110 | –0.0093 | 0.0017 | 0.0505 | –4.0 (–4.7) |

We analyzed whether charge transfer effects are also similar in all trimers by using the natural bond orbital (NBO) analysis. The results are shown in **Figure 10**, demonstrating the LP(N)→σ(C–I) charge transfer that is typical in the σ-hole interactions. The stabilization energies obtained from the second order perturbation analysis are given in red, evidencing that they are very similar in both types of HaBs in **3**·½(1,4-FIB) and smaller in AdCN·½(1,4-FIB), in line with the MEP and QTAIM analyses results.

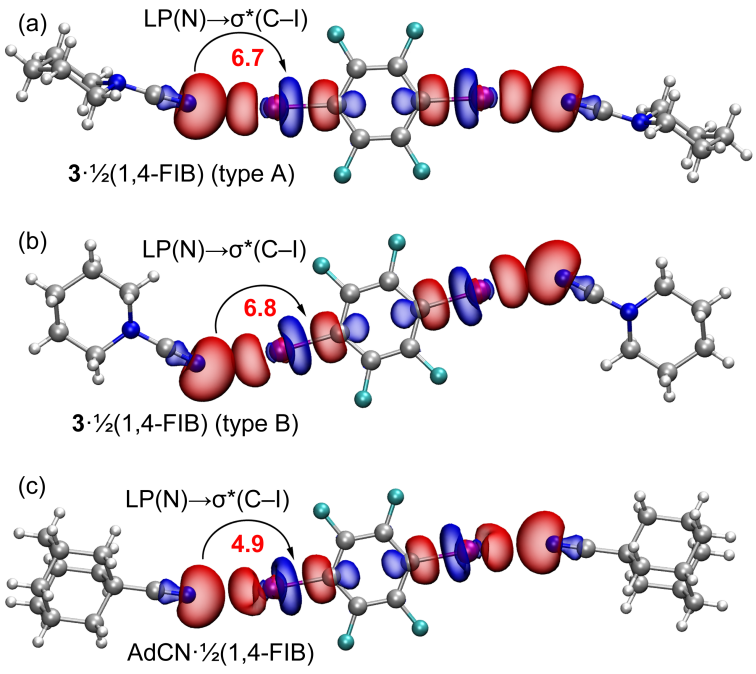

**Figure 10**. NBOs involved in the orbital charge transfer in **3**·½(1,4-FIB) type A (a), **3**·½(1,4-FIB) type B (b), and AdCN·½(1,4-FIB) (c) cocrystals. The $E^{(2)}$ energies are given in red.

Finally, we performed an energy decomposition analysis to better understand the similar binding energy observed for the HaBs in the structures of **3**·½(1,4-FIB) and AdCN·½(1,4-FIB). We computed HaB dimers of **3**·½(1,4-FIB) type A and AdCN·½(1,4-FIB) and obtained the exchange repulsion ($E_{ex\text{-}rep}$), electrostatic ($E_{el}$), orbital ($E_{orb}$), correlation ($E_{cor}$), and dispersion ($E_{disp}$) components to the total ($E_{tot}$) interaction energy (**Figure 11**). The interaction energies for both dimers are quite similar, –6.15 kcal/mol for **3**·½(1,4-FIB) type A and –5.58 kcal/mol for AdCN·½(1,4-FIB), as previously observed for the trimers. As expected, based on the comparison of the relative basicity of cyanamides and nitriles, all attractive components are more negative (favorable) for the cyanamide heterodimer, especially electrostatics ($E_{el}$) and orbital ($E_{orb}$) contributions. The differences observed in the correlation and dispersion terms are smaller (<1 kcal/mol). The most significant difference between both dimers consists of the exchange-repulsion contribution that is significantly larger (repulsive) in the cyanamide cocrystal. This is likely due to the very short distance in the **3**·½(1,4-FIB) type A that has a large effect on the Pauli repulsion term, thus compensating the other attractive terms and explaining the small difference in the binding energies of **3**·½(1,4-FIB) and AdCN·½(1,4-FIB).

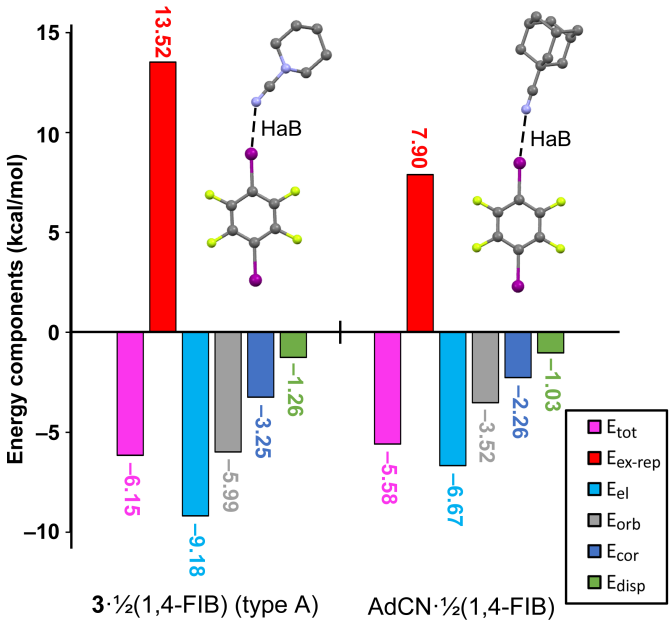


**Figure 11**. Total ($E_{tot}$), exchange-repulsion ($E_{ex\text{-}rep}$), electrostatic ($E_{el}$), correlation ($E_{cor}$), dispersion ($E_{disp}$), and orbital ($E_{orb}$) energetic terms for the dimers of **3**·½(1,4-FIB) type A and AdCN·½(1,4-FIB) in kcal/mol using the Kitaura–Morokuma analysis.

## Conclusions

Cocrystals **1**·1,3,5-FIB, **2**·1,3,5-FIB, **3**·½(1,4-FIB), and **4**·2(1,3,5-FIB) were derived from the association of push-pull nitriles $NCNR_2$ (**1**–**4**) and iodo-substituted perfluorobenzenes (1,3,5-FIB and 1,4-FIB). The supramolecular organization of all these structures is primarily determined by the I··· $N_{nitrile}$ halogen bonding. This type of rare I···*sp*-N interaction has been earlier recognized for conventional nitriles NCR (R = Alk, Ar), functioning as HaB acceptors, but never reported for push-pulling nitriles, including dialkylcyanamides. In this study, we compared I···*sp*-N HaBs involving the conventional nitrile AdCN (in AdCN·½(1,4-FIB)) and the push-pulling dialkylcyanamide, $NCNC_5H_{10}$ (in **3**·½(1,4-FIB)), and revealed significant similarity between the HaB situations in these two structures. Although AdCN is slightly poorer *sp*-N electron donor than the push-pull nitrile $NCNC_5H_{10}$ (**3**), HaBs in the cocrystals exhibit similar interaction energies. The stabilization energy for LP(N)→σ(C–I) charge transfer is only slightly smaller in

AdCN·½(1,4-FIB) than in **3**·½(1,4-FIB). Furthermore, the likeness of the HaB binding energies in the two structures was supported by the results of the energy decomposition analysis. Summarizing our comparative data, one can conclude that the noncovalent bonding (based, first of all, on electrostatic interactions) leads to a leveling effect for the HaBs of these two types of nitrile compounds.

It is noteworthy that HaBs involving a nitrile-group found its application in the property control of crystalline materials: HaB-induced luminescence in solid gold(I) complexes,[42] blue-shifted luminescence emission in HaB-based organic cocrystals,[38] and also a structure-determining force for the supramolecular architecture of iodophthalodinitrile species.[39] Considering the similarities of the HaBs involving conventional and push-pull nitriles, one should expect that dialkylcyanamides could also serve as potent HaB acceptors for crystal engineering and targeted design of extended solid architectures. Works in this direction are underway in our group.

## 5. Experimental Section

**5.1. Materials and instrumentation.** All reagents and solvents were obtained from commercial sources and used as received.

**5.2. Cocrystal growth.** Co-crystallizations of **1**·1,3,5-FIB, **2**·1,3,5-FIB, **3**·½(1,4-FIB), **4**·½(1,4-FIB), and **4**·2(1,3,5-FIB) were performed on dissolution of any one of the HaB donors (0.1 mmol; 40.2 mg for 1,4-FIB; 51.0 mg for 1,3,5-FIB) and 3-fold excess of $NCNR_2$ (0.3 mmol; 21.0 mg for $R_2 = Me_2$ **1**, 28.3 mg for $C_4H_8$ **2**, 33.1 mg for $C_5H_{10}$ **3**, 33.6 mg for $C_4H_8O$ **4**) in MeCN (2 mL); the homogenization was stimulated by using an ultrasound bath. The reaction mixture was left to stand for 3–5 days at 20–22 °C for slow evaporation (3–5 days) to dryness. Colorless crystals of **1**·1,3,5-FIB, **2**·1,3,5-FIB, **3**·½(1,4-FIB), **4**·½(1,4-FIB), and **4**·2(1,3,5-FIB) (yields 40–70%) were separated mechanically and studied by XRD and ATR-IR methods.

**5.3. X-ray structure determinations**. XRD studies were performed at 100 K on XtaLAB Synergy, Single source at home/near, HyPix diffractometer using monochromated CuKα (λ = 1.54184 Å)

radiation. The structures were solved by the ShelXT[58] structure solution program using Intrinsic Phasing and refined with the ShelXL[59] refinement package incorporated in the OLEX2 program package[60] using least-squares minimization. Empirical absorption correction was applied in the CrysAlis Pro program complex using spherical harmonics implemented in SCALE3 ABSPACK scaling algorithm.

**5.4 Theoretical methods.** The calculations were performed using the Turbomole program 7.7[61] at the PBE0-D3/def2-TZVP level of theory.[62-65] The MEP surfaces were plotted using the 0.001 a.u. isosurface. The QTAIM[66] and NCIPlot[67] analyses were represented using the VMD software.[68] The Multiwfn program[69] was used for the QTAIM and NCIplot calculations. The following settings were used to represent the NCIplot in the Figures of this manuscript: RDG = 0.5, ρ cut-off = 0.04 a.u. color code –0.03 a.u. ≤ (sign$\lambda_2$)ρ ≤ 0.03 a.u. The natural bond orbital (NBO) analysis[70] was performed using the NBO7 program.[71] The EDA analysis was performed using the Kitaura–Morokuma method[72] as implemented in Turbomole 7.7 program.

## ASSOCIATED CONTENT

### Supporting Information

The Supporting Information is available free of charge at HYPERLINK. The CSD search, crystal data and structure refinement, IR spectra, Hirshfeld surface analysis, NBO analysis

### Accession Codes

CCDC 2280379; 2280380; 2280376; 2280378; 2280385 contain the supplementary crystallographic data for this paper. These data can be obtained free of charge via www.ccdc.cam.ac.uk/data_request/cif, or by emailing data_request@ccdc.cam.ac. or by contacting The Cambridge Crystallographic Data Centre, 12 Union Road, Cambridge CB2 1EZ, UK; fax: +44 1223 336033.

## AUTHOR INFORMATION


### Corresponding Author

**Vadim Yu. Kukushkin** – *Institute of Chemistry, Saint Petersburg State University, 7/9 Universitetskaya Nab., Saint Petersburg 199034, Russian Federation; Laboratory of Crystal Engineering of Functional Materials, South Ural State University, 76 Lenin Av., Chelyabinsk 454080, Russian Federation*; orcid.org/0000-0002-2253-085X; Email: v.kukushkin@spbu.ru

**Nadezhda A. Bokach** – *Institute of Chemistry, Saint Petersburg State University, 7/9 Universitetskaya Nab., Saint Petersburg 199034, Russian Federation*; orcid.org/0000-0001-8692-9627; Email: n.bokach@spbu.ru

### Authors

**Yulia N. Toikka** – *Institute of Chemistry, Saint Petersburg State University, 7/9 Universitetskaya Nab., Saint Petersburg 199034, Russian Federation*

**Rosa M. Gomila** – *Department of Chemistry, Universitat de les Illes Balears, Crta de Valldemossa km 7.5, 07122 Palma de Mallorca (Baleares), Spain*; orcid.org/0000-0002-0827-8504

**Antonio Frontera** – *Department of Chemistry, Universitat de les Illes Balears, Crta de Valldemossa km 7.5, 07122 Palma de Mallorca (Baleares), Spain*; orcid.org/0000-0001-7840-2139

**Yulia A. Izotova** – *Institute of Chemistry, Saint Petersburg State University, 7/9 Universitetskaya Nab., Saint Petersburg 199034, Russian Federation*

Complete contact information is available at: HYPERLINK.


### Notes

The authors declare no competing financial interest.

**ACKNOWLEDGEMENTS**

This article is written in commemoration of the 300th anniversary of Saint Petersburg State University's founding. VYK thanks the Russian Science Foundation for support of this study (grant 23-13-00033). Authors are much obliged to the Center for X-ray Diffraction Studies (belonging to Saint Petersburg State University) for XRD measurements and the Center for Chemical Analysis and Materials Research for physicochemical studies.

## REFERENCES


1. Odd Hassel – Nobel Lecture. <https://www.nobelprize.org/prizes/chemistry/1969/hassel/lecture/> (accessed Mon. 29 May 2023.).
2. Desiraju, G. R.; Ho, P. S.; Kloo, L.; Legon, A. C.; Marquardt, R.; Metrangolo, P.; Politzer, P.; Resnati, G.; Rissanen, K., Definition of the halogen bond (IUPAC Recommendations 2013). *Pure Appl. Chem.* **2013**, *85*, 1711.
3. Brammer, L.; Peuronen, A.; Roseveare, T. M., Halogen bonds, chalcogen bonds, pnictogen bonds, tetrel bonds and other [sigma]-hole interactions: a snapshot of current progress. *Acta Crystallographica Section C* **2023**, *79*, 204-216.
4. von der Heiden, D.; Vanderkooy, A.; Erdelyi, M., Halogen bonding in solution: NMR spectroscopic approaches. *Coord. Chem. Rev.* **2020**, *407*, 213147.
5. Tepper, R.; Schubert, U. S., Halogen Bonding in Solution: Anion Recognition, Templated Self-Assembly, and Organocatalysis. *Angew. Chem. Int. Ed.* **2018**, *57*, 6004-6016.
6. Wang, H.; Wang, W. Z.; Jin, W. J., sigma-Hole Bond vs pi-Hole Bond: A Comparison Based on Halogen Bond. *Chem. Rev.* **2016**, *116*, 5072-5104.
7. Kolar, M. H.; Hobza, P., Computer Modeling of Halogen Bonds and Other sigma-Hole Interactions. *Chem. Rev.* **2016**, *116*, 5155-5187.
8. Cavallo, G.; Metrangolo, P.; Milani, R.; Pilati, T.; Priimagi, A.; Resnati, G.; Terraneo, G., The Halogen Bond. *Chem. Rev.* **2016**, *116*, 2478-2601.
9. Bauza, A.; Mooibroek, T. J.; Frontera, A., The Bright Future of Unconventional sigma/-Hole Interactions. *ChemPhysChem* **2015**, *16*, 2496-2517.
10. Gilday, L. C.; Robinson, S. W.; Barendt, T. A.; Langton, M. J.; Mullaney, B. R.; Beer, P. D., Halogen Bonding in Supramolecular Chemistry. *Chem. Rev.* **2015**, *115*, 7118-7195.
11. Mukherjee, A.; Tothadi, S.; Desiraju, G. R., Halogen Bonds in Crystal Engineering: Like Hydrogen Bonds yet Different. *Acc. Chem. Res.* **2014**, *47*, 2514-2524.
12. Priimagi, A.; Cavallo, G.; Metrangolo, P.; Resnati, G., The Halogen Bond in the Design of Functional Supramolecular Materials: Recent Advances. *Acc. Chem. Res.* **2013**, *46*, 2686-2695.
13. Scholfield, M. R.; Vander Zanden, C. M.; Carter, M.; Ho, P. S., Halogen bonding (X-bonding): A biological perspective. *Protein Sci.* **2013**, *22*, 139-152.
14. Taylor, M. S., Anion recognition based on halogen, chalcogen, pnictogen and tetrel bonding. *Coordination Chemistry Reviews* **2020**, *413*, 213270.
15. Il'in, M. V.; Sysoeva, A. A.; Novikov, A. S.; Bolotin, D. S., Diaryliodoniums as Hybrid Hydrogen- and Halogen-Bond-Donating Organocatalysts for the Groebke-Blackburn-Bienayme Reaction. *J. Org. Chem.* **2022**, *87*, 4569-4579.
16. Riel, A. M. S.; Decato, D. A.; Sun, J.; Berryman, O. B., Halogen bonding organocatalysis enhanced through intramolecular hydrogen bonds. *Chem. Commun.* **2022**, *58*, 1378-1381.
17. Benito, I.; Gomila, R. M.; Frontera, A., On the energetic stability of halogen bonds involving metals: implications in crystal engineering. *CrystEngComm* **2022**, *24*, 4440-4446.
18. Ahangar, A. A.; Elancheran, R.; Dar, A. A., Influence of halogen substitution on crystal packing, molecular properties and electrochemical sensing. *J. Solid State Chem.* **2022**, *314*, 123382.
19. Soldatova, N. S.; Postnikov, P. S.; Ivanov, D. M.; Semyonov, O. V.; Kukurina, O. S.; Guselnikova, O.; Yamauchi, Y.; Wirth, T.; Zhdankin, V. V.; Yusubov, M. S.; Gomila, R. M.; Frontera, A.; Resnati, G.; Kukushkin, V. Y., Zwitterionic iodonium species afford halogen bond-based porous organic frameworks. *Chem. Sci.* **2022**, *13*, 5650-5658.
20. Ball, M. L.; Milic, J. V.; Loo, Y.-L., The Emerging Role of Halogen Bonding in Hybrid Perovskite Photovoltaics. *Chem. Mater.* **2022**, *34*, 2495-2502.

21. Dai, W.; Niu, X.; Wu, X.; Ren, Y.; Zhang, Y.; Li, G.; Su, H.; Lei, Y.; Xiao, J.; Shi, J.; Tong, B.; Cai, Z.; Dong, Y., Halogen Bonding: A New Platform for Achieving Multi-Stimuli-Responsive Persistent Phosphorescence. *Angew. Chem., Int. Ed.* **2022**, *61*, e202200236.
22. Juneja, N.; Shapiro, N. M.; Unruh, D. K.; Bosch, E.; Groeneman, R. H.; Hutchins, K. M., Controlling Thermal Expansion in Supramolecular Halogen-Bonded Mixed Cocrystals through Synthetic Feed and Dynamic Motion. *Angew. Chem., Int. Ed.* **2022**, *61*, e202202708.
23. Metrangolo, P.; Canil, L.; Abate, A.; Terraneo, G.; Cavallo, G., Halogen Bonding in Perovskite Solar Cells: A New Tool for Improving Solar Energy Conversion. *Angew. Chem., Int. Ed.* **2022**, *61*, e202114793.
24. Yang, X.-G.; Zhang, Y.; Wang, W.; Ma, L.-F., Enhanced Optoelectronic Performances of the Cocrystals between 2,2′-Bi(1,8-naphthyridine) and Iodine through Strong Halogen Bonds. *Cryst. Growth Des.* **2022**, *22*, 6863-6869.
25. Kang, Y.; Dong, Y.; Liu, Y.; Gao, H.; Wang, Y.; Shreeve, J. n. M., Halogen bonding (C-F···X) and its effect on creating ideal insensitive energetic materials. *Chem. Eng. J.* **2022**, *440*, 135969.
26. Hein, R.; Beer, P. D., Halogen bonding and chalcogen bonding mediated sensing. *Chem. Sci.* **2022**, *13*, 7098-7125.
27. Barragan, A.; Lois, S.; Sarasola, A.; Vitali, L., Empowering non-covalent hydrogen, halogen, and [S-N]2 bonds in synergistic molecular assemblies on Au(111). *Nanoscale* **2022**, *14*, 17895-17899.
28. Mu, K.; Zhu, Z.; Abula, A.; Peng, C.; Zhu, W.; Xu, Z., Halogen Bonds Exist between Noncovalent Ligands and Natural Nucleic Acids. *J. Med. Chem.* **2022**, *65*, 4424-4435.
29. Saha, S.; Desiraju, G. R., σ-Hole and π-Hole Synthon Mimicry in Third-Generation Crystal Engineering: Design of Elastic Crystals. *Chemistry – A European Journal* **2017**, *23*, 4936-4943.
30. Politzer, P.; Murray, J. S., Electrostatics and Polarization in σ- and π-Hole Noncovalent Interactions: An Overview. *ChemPhysChem* **2020**, *21*, 579-588.
31. Tarannam, N.; Shukla, R.; Kozuch, S., Yet another perspective on hole interactions. *Physical Chemistry Chemical Physics* **2021**, *23*, 19948-19963.
32. Frontera, A.; Bauzá, A., On the Importance of σ–Hole Interactions in Crystal Structures. *Crystals* **2021**, *11*, 1205.
33. Ivanov, D. M.; Novikov, A. S.; Ananyev, I. V.; Kirina, Y. V.; Kukushkin, V. Y., Halogen bonding between metal centers and halocarbons. *Chem. Commun.* **2016**, *52*, 5565-5568.
34. Cavallo, G.; Metrangolo, P.; Milani, R.; Pilati, T.; Priimagi, A.; Resnati, G.; Terraneo, G., The Halogen Bond. *Chemical Reviews* **2016**, *116*, 2478-2601.
35. Blackstock, S. C.; Lorand, J. P.; Kochi, J. K., Charge-transfer interactions of amines with tetrahalomethanes. X-ray crystal structures of the donor-acceptor complexes of quinuclidine and diazabicyclo [2.2.2]octane with carbon tetrabromide. *The Journal of Organic Chemistry* **1987**, *52*, 1451-1460.
36. Raatikainen, K.; Rissanen, K., Interaction between amines and N-haloimides: a new motif for unprecedentedly short Br···N and I···N halogen bonds. *CrystEngComm* **2011**, *13*, 6972-6977.
37. Metrangolo, P.; Pilati, T.; Resnati, G.; Stevenazzi, A., Metric engineering of perfluorocarbon–hydrocarbon layered solids driven by the halogen bonding. *Chemical Communications* **2004**, 1492-1493.
38. Yan, D.; Delori, A.; Lloyd, G. O.; Friščić, T.; Day, G. M.; Jones, W.; Lu, J.; Wei, M.; Evans, D. G.; Duan, X., A Cocrystal Strategy to Tune the Luminescent Properties of Stilbene-Type Organic Solid-State Materials. *Angewandte Chemie International Edition* **2011**, *50*, 12483-12486.
39. Ateş, Ö. D.; Zorlu, Y.; Kanmazalp, S. D.; Chumakov, Y.; Gürek, A. G.; Ayhan, M. M., Halogen bonding driven crystal engineering of iodophthalonitrile derivatives. *CrystEngComm* **2018**, *20*, 3858-3867.

40. Giordano, N.; Afanasjevs, S.; Beavers, C. M.; Hobday, C. L.; Kamenev, K. V.; O'Bannon, E. F.; Ruiz-Fuertes, J.; Teat, S. J.; Valiente, R.; Parsons, S., The Effect of Pressure on Halogen Bonding in 4-Iodobenzonitrile. *Molecules* **2019**, *24*, 2018.
41. Gamekkanda, J. C.; Sinha, A. S.; Desper, J.; Đaković, M.; Aakeröy, C. B., The Role of Halogen Bonding in Controlling Assembly and Organization of Cu(II)-Acac Based Coordination Complexes. *Crystals* **2017**, *7*, 226.
42. Wang, M.-J.; Wang, Z.-Y.; Luo, P.; Li, B.; Wang, L.-Y.; Zang, S.-Q., Recoverable Mechanoresponsive Luminescent Molecular Sponge Material: A Novel Aryl Gold(I) Isocyanide Compound. *Crystal Growth & Design* **2019**, *19*, 538-542.
43. Scheiner, S., Halogen Bonds Formed between Substituted Imidazoliums and N Bases of Varying N-Hybridization. *Molecules* **2017**, *22*, 1634.
44. Raczyńska, E. D.; Gal, J.-F.; Maria, P.-C., Enhanced Basicity of Push–Pull Nitrogen Bases in the Gas Phase. *Chemical Reviews* **2016**, *116*, 13454-13511.
45. Smirnov, A. S.; Butukhanova, E. S.; Bokach, N. A.; Starova, G. L.; Gurzhiy, V. V.; Kuznetsov, M. L.; Kukushkin, V. Y., Novel (cyanamide)ZnII complexes and zinc(ii)-mediated hydration of the cyanamide ligands. *Dalton Transactions* **2014**, *43*, 15798-15811.
46. Smirnov, A. S.; Yandanova, E. S.; Bokach, N. A.; Starova, G. L.; Gurzhiy, V. V.; Avdontceva, M. S.; Zolotarev, A. A.; Kukushkin, V. Y., Zinc(ii)-mediated generation of 5-amino substituted 2,3-dihydro-1,2,4-oxadiazoles and their further ZnII-catalyzed and O2-involving transformations. *New Journal of Chemistry* **2015**, *39*, 9330-9344.
47. Bikbaeva, Z. M.; Novikov, A. S.; Suslonov, V. V.; Bokach, N. A.; Kukushkin, V. Y., Metal-mediated reactions between dialkylcyanamides and acetamidoxime generate unusual (nitrosoguanidinate)nickel(ii) complexes. *Dalton Transactions* **2017**, *46*, 10090-10101.
48. Bokach, N. A.; Kukushkin, V. Y., Coordination chemistry of dialkylcyanamides: Binding properties, synthesis of metal complexes, and ligand reactivity. *Coordination Chemistry Reviews* **2013**, *257*, 2293-2316.
49. Dang, L.; Yang, H., Crystal structure of 18-crown-6 – 1,4-diiodotetrafluorobenzene – acetonitrile (1/1/2), C22H30F4I2N2O6. *Zeitschrift für Kristallographie - New Crystal Structures* **2020**, *235*, 663-664.
50. Wasilewska, A.; Gdaniec, M.; Polonski, T., CCDC 618388: Experimental Crystal Structure Determination. *CSD Communication* **2016**, 618388.
51. Szell, P. M. J.; Gabriel, S. A.; Caron-Poulin, E.; Jeannin, O.; Fourmigué, M.; Bryce, D. L., Cosublimation: A Rapid Route Toward Otherwise Inaccessible Halogen-Bonded Architectures. *Crystal Growth & Design* **2018**, *18*, 6227-6238.
52. Wright, K.; Drouillat, B.; Menguy, L.; Marrot, J.; Couty, F., The von Braun Reaction Applied to Azetidines. *European Journal of Organic Chemistry* **2017**, *2017*, 7195-7201.
53. Ivanov, D. M.; Novikov, A. S.; Starova, G. L.; Haukka, M.; Kukushkin, V. Y., A family of heterotetrameric clusters of chloride species and halomethanes held by two halogen and two hydrogen bonds. *CrystEngComm* **2016**, *18*, 5278-5286.
54. Bondi, A., van der Waals Volumes and Radii. *J. Phys. Chem.* **1964**, *68*, 441-451.
55. Eliseeva, A. A.; Ivanov, D. M.; Novikov, A. S.; Kukushkin, V. Y., Recognition of the π-hole donor ability of iodopentafluorobenzene – a conventional σ-hole donor for crystal engineering involving halogen bonding. *CrystEngComm* **2019**, *21*, 616-628.
56. Saha, B. K.; Veluthaparambath, R. V. P.; Krishna G., V., Halogen···Halogen Interactions: Nature, Directionality and Applications. *Chemistry – An Asian Journal* **2023**, *18*, e202300067.
57. Bartashevich, E. V.; Tsirelson, V. G., Interplay between non-covalent interactions in complexes and crystals with halogen bonds. *Russian Chemical Reviews* **2014**, *83*, 1181.
58. Sheldrick, G., SHELXT - Integrated space-group and crystal-structure determination. *Acta Cryst. Sect. A* **2015**, *71*, 3-8.
59. Sheldrick, G., Crystal structure refinement with SHELXL. *Acta Crystallographica Section C* **2015**, *71*, 3-8.

60. Dolomanov, O. V.; Bourhis, L. J.; Gildea, R. J.; Howard, J. A.; Puschmann, H., OLEX2: a complete structure solution, refinement and analysis program. *J. Appl. Crystallogr.* **2009**, *42*, 339-341.
61. Ahlrichs, R.; Bär, M.; Häser, M.; Horn, H.; Kölmel, C., Electronic structure calculations on workstation computers: The program system turbomole. *Chemical Physics Letters* **1989**, *162*, 165-169.
62. Adamo, C.; Barone, V., Toward reliable density functional methods without adjustable parameters: The PBE0 model. *The Journal of Chemical Physics* **1999**, *110*, 6158-6170.
63. Grimme, S.; Antony, J.; Ehrlich, S.; Krieg, H., A consistent and accurate ab initio parametrization of density functional dispersion correction (DFT-D) for the 94 elements H-Pu. *The Journal of Chemical Physics* **2010**, *132*, 154104.
64. Weigend, F., Accurate Coulomb-fitting basis sets for H to Rn. *Physical Chemistry Chemical Physics* **2006**, *8*, 1057-1065.
65. Weigend, F.; Ahlrichs, R., Balanced basis sets of split valence, triple zeta valence and quadruple zeta valence quality for H to Rn: Design and assessment of accuracy. *Physical Chemistry Chemical Physics* **2005**, *7*, 3297-3305.
66. Bader, R. F. W., A quantum theory of molecular structure and its applications. *Chemical Reviews* **1991**, *91*, 893-928.
67. Contreras-García, J.; Johnson, E. R.; Keinan, S.; Chaudret, R.; Piquemal, J.-P.; Beratan, D. N.; Yang, W., NCIPLOT: A Program for Plotting Noncovalent Interaction Regions. *Journal of Chemical Theory and Computation* **2011**, *7*, 625-632.
68. Humphrey, W.; Dalke, A.; Schulten, K., VMD: Visual molecular dynamics. *Journal of Molecular Graphics* **1996**, *14*, 33-38.
69. Lu, T.; Chen, F., Multiwfn: A multifunctional wavefunction analyzer. *Journal of Computational Chemistry* **2012**, *33*, 580-592.
70. Glendening, E. D.; Landis, C. R.; Weinhold, F., Natural bond orbital methods. *WIREs Computational Molecular Science* **2012**, *2*, 1-42.
71. Glendening, E. D.; Badenhoop, J. K.; Reed, A. E.; Carpenter, J. E.; Bohmann, J. A.; Morales, C. M.; Karafiloglou, P.; Landis, C. R.; F., W. *NBO 7.0.*, Theoretical Chemistry Institute, University of Wisconsin, Madison, WI., 2018.
72. Kitaura, K.; Morokuma, K., A new energy decomposition scheme for molecular interactions within the Hartree-Fock approximation. *International Journal of Quantum Chemistry* **1976**, *10*, 325-340.

**For Table of Contents Use Only**

# Push-Pull and Conventional Nitriles as Halogen Bond Acceptors in Cocrystals with Iodo-substituted Perfluorobenzenes

Yulia N. Toikka,[1] Rosa M. Gomila,[2] Antonio Frontera,[2] Vadim Yu. Kukushkin,*[1,3]

Nadezhda A. Bokach*[1]

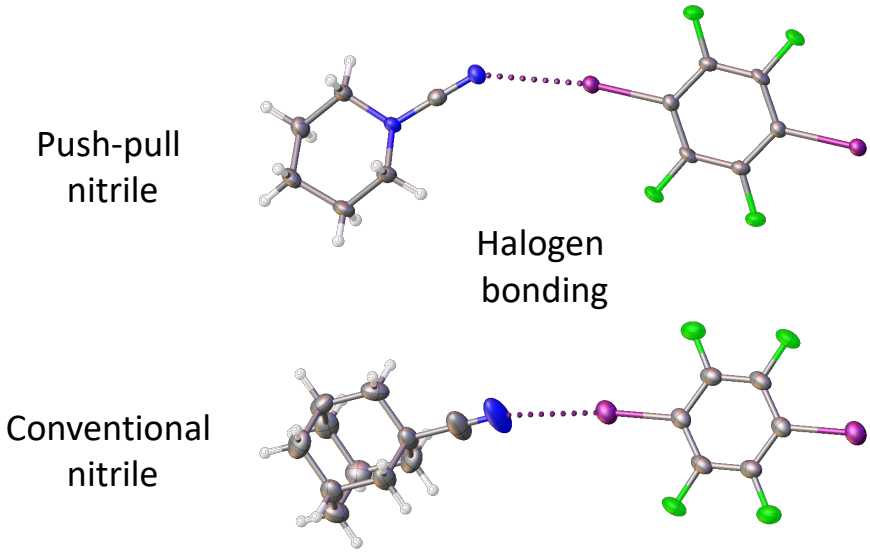


Significant similarity between the I···*sp*-N interaction for conceptually different push-pull and conventional nitriles in their role of halogen bond acceptors.